# Comprehensive screening of a light-inducible split Cre recombinase with domain insertion profiling

Nathan Tague[1,2], Virgile Andreani[1,2], Yunfan Fan[3], Winston Timp[3,4], Mary J. Dunlop[1,2]*

[1] Department of Biomedical Engineering, Boston University, Boston, MA, USA 02215
[2] Biological Design Center, Boston University, Boston, MA, USA 02215
[3] Department of Biomedical Engineering, Johns Hopkins University, Baltimore, MD, USA
[4] Department of Molecular Biology and Genetics, Johns Hopkins University, Baltimore, MD, USA
* Corresponding author: mjdunlop@bu.edu

## Abstract

Splitting proteins with light- or chemically-inducible dimers provides a mechanism for post-translational control of protein function. However, current methods for engineering stimulus-responsive split proteins often require significant protein engineering expertise and laborious screening of individual constructs. To address this challenge, we use a pooled library approach that enables rapid generation and screening of nearly all possible split protein constructs in parallel, where results can be read out using sequencing. We perform our method on Cre recombinase with optogenetic dimers as a proof of concept, resulting in comprehensive data on split sites throughout the protein. To improve accuracy in predicting split protein behavior, we develop a Bayesian computational approach to contextualize errors inherent to experimental procedures. Overall, our method provides a streamlined approach for achieving inducible post-translational control of a protein of interest.

## Keywords

split proteins, domain insertion profiling, optogenetics, Cre recombinase, Bayesian inference, protein engineering

## Introduction

The ability to control protein function is important for gaining insight into native biological systems and also engineering novel synthetic functions. Chemical inducers enable dose-responsive regulation of protein activity in response to small molecules, thus offering a versatile means of control. Optogenetic control offers an additional level of functionality since light can provide a reversible and precise input to enable temporal control over protein function. Both chemosensory and optogenetic approaches have been widely used in diverse fields ranging from biological discovery to engineering.[1–10]

Signal response times are particularly important for optogenetic protein tools because primary use cases center around controlling temporal changes.[11–15] Because of this, post-translational mechanisms offer an attractive option for synthetic tools, because they avoid time delays associated with transcription and translation. Several studies have achieved post-translational control by splitting proteins with stimulus-responsive dimers.[2,7,16] In the case of post-translational optogenetic control, light-responsive dimers are commonly used.[17–20] In this approach, proteins are translated in two separate halves that are inactive. Each half is fused with a light-responsive dimer, which dimerize in response to light exposure. For example, Nihongaki *et al*. introduced a Cas9 split with optogenetic dimers that can perform RNA-guided gene edits or gene repression in response to light.[10] The split site where the optogenetic domains are incorporated within the protein of interest determines if the design is light-responsive, leaky, or non-functional. Deciding where to split the protein is often challenging, necessitating laborious screening of many split sites chosen based on structural information to find a functional construct.[7,10,21] Computation approaches exist to predict functional split sites, which can assist in choosing candidates for testing.[22] However, these models are not always accurate and do not take into account the dimer domains used, which can influence split site functionality.[21]

In principle, the challenge of identifying where to insert optogenetic domains is more tractable and limited in scope in comparison to other protein engineering endeavors, such as mutagenesis screens or directed evolution studies. The number of constructs to test is on the order of the number of amino acids in the protein of interest (hundreds to thousands). Consequently, we reasoned that the challenge of identifying functional split sites could be addressed efficiently with a parallelized approach by screening all possible split sites in a pooled library (Fig. 1).

To simplify the library construction process, we used a pooled approach to generate variants with proteins split at all possible sites. Mahdavi *et al*. demonstrated that split libraries can be generated and screened with transposon mutagenesis.[23] However, their work identifies split proteins that spontaneously combine, which is valuable in certain contexts, but not ideal for post-translation control of protein function. In order to generate libraries capable of input-responsiveness, domains also need to be inserted into the protein of interest with minimal scarring to facilitate functional translation and folding. Nadler *et al.* created a library generation method called domain insertion profiling combined with sequencing, or DIP-seq, that utilizes a MuA transposase to insert a modified transposon randomly within a sequence of interest (Fig. 2a).[24] The transposon contains a chloramphenicol resistance ($Cm^R$) gene flanked by BsaI sites, a type IIS restriction enzyme site that allows the $Cm^R$ sequence to be swapped out for a desired insertion sequence at a later stage. This cloning scheme generates a library of constructs where a domain is inserted comprehensively into a plasmid to create a transposon insertion library. To isolate insertions that are within the gene encoding the protein of interest, BsmBI restriction enzyme sites flanking the region are used to excise the sequence and clone it into an expression vector using a golden gate reaction[25] to create an expression library. The transposon fragment within these plasmids is then replaced with the domain that will be incorporated into the protein of interest. In their study, Nadler *et al.* inserted a fluorescent protein domain into a protein that binds trehalose to create a fluorescent biosensor.[24] We reasoned that the DIP-seq technique could be modified to create split protein libraries by instead inserting two dimerization domains with an internal ribosome binding sequence (RBS), such that the resulting constructs are expressed as two proteins (Fig. 2b).

Here, we demonstrate this method of creating and screening split proteins in pooled libraries. As a proof of concept, we profiled split sites for Cre recombinase, a widely-used protein in genetics and synthetic biology that enables site-specific gene recombination, inversion, or excision.[26,27] We split Cre and inserted light-responsive dimer domains, called ‘magnets’,[20] and comprehensively profiled for activity in response to blue light. We then used pooled sequencing to link split site library distributions to functional behavior of individual split proteins. To analyze the datasets output from our workflow, we designed a Bayesian inference approach to output predictions on the functionality of individual split sites. This approach is capable of managing several sources of error that arise experimentally, such as heterogeneous library distribution and spurious cell sorting events, and provides a probabilistic prediction about whether a given split site is likely to be a functional hit. We validated the approach by individually characterizing several split proteins that the model predicted to be hits, leaky variants that are not light-responsive, or non-functional results. In sum, we describe a method to create post-translational optogenetic control. This approach should be generalizable to other proteins or inducible dimer domains of interest.

## Results

### *Design of parallel split Cre screening*

To create a split Cre recombinase library, we applied the modified domain insertion approach to construct a staging plasmid containing the Cre coding sequence with a 17 amino acid N-terminal truncation as described in Jullien *et al.*[2] (Tables S1-S3). We created a transposon insertion library by integrating the modified transposon randomly into a Cre staging plasmid using MuA transposase, as described above (Fig. 2a-b). Once the Cre-transposon fragment was cloned into an expression vector, the transposon sequence was replaced by an insertion fragment containing the optogenetic 'magnet' heterodimers (pMag and nMagHigh1) with an RBS between the dimers (Fig. 2c).[20] The insertion fragment was designed such that, when inserted in-frame, glycine-serine linkers are incorporated between the Cre coding sequence and each magnet (Table S2-S3). A five-nucleotide sequence from Cre is duplicated during the transposon reaction and the insert fragment was designed to maintain an open reading frame for the N-terminal and C-terminal split Cre fragments (Fig. S1). Sequencing of the initial split Cre expression library confirmed that the Cre sequence was comprehensively split, with >85% (282 out of 326 codons) of total split possibilities present (Table S4).

As a readout to measure recombination activity, we designed the expression vector to contain a fluorescent reporter (Fig. 2c). The reporter contains a transcriptional terminator flanked by *loxP* sites placed in between a constitutive promoter and the gene encoding superfolder GFP (*sfgfp*). Without active Cre, the terminator blocks transcription of *sfgfp*. Cre-mediated recombination excises the terminator resulting in a 129-fold increase in green fluorescence (Fig. 2d).

Using our expression library containing Cre recombinase split at the majority of amino acids, we next subjected the library to an experimental workflow devised to test the behavior of each variant of split Cre in parallel (Fig. 2e). Since the expression plasmid contains a fluorescent reporter for Cre activity, the activity of a given split Cre variant can be linked to the sequence that generated the cutting. Using fluorescence-activated cell sorting (FACS), we sorted cells based on Cre activity and sequenced the plasmid populations to determine which split Cre variants were present. Specifically, we divided the pooled library into two equal parts and subjected one to blue light exposure while the other was kept in the dark. Using FACS, we separated cells that expressed GFP (denoted +GFP) and from those that did not (-GFP) for each light treatment condition. By treating the library with blue light or keeping it in the dark prior to sorting, we reasoned that we could compare populations to determine which split sites were light-responsive (Fig. 2e). We performed next generation sequencing on each of the four libraries (Light/+GFP, Light/-GFP, Dark/+GFP, Dark/-GFP) and filtered for reads that contained the interface between the Cre coding sequence and either pMag or nMagHigh1 to identify the split protein variants present in each library. Counts for these filtered reads were greater than $10^4$ for each of the four libraries (Table S4).

*Experimental error and Bayesian modeling*

We considered three possible phenotypes for each split Cre variant: a hit (active in the light but not in the dark), leaky (active even in the dark), or non-functional (inactive in the light and the dark) (Fig. S2). Our initial hypothesis was that by comparing the Light/+GFP population to the Dark/+GFP population, it would be straightforward to identify hits. However, initial attempts at analyzing these populations through simple measures, such as dividing the proportion of each split site in the Light population by the proportion in the Dark population to identify hits proved inaccurate. Simple analysis measures like this were prone to false positive hit predictions stemming from low coverage of certain sites due to low sequencing read counts associated with some split variants, with low or null read counts on either Light or Dark populations strongly affecting these ratiometric calculations. Therefore, we examined our experimental workflow for sources of error that could be causing inaccurate predictions and identified three major factors that can contribute to error. First, variants are represented in the naïve libraries prior to cell sorting with widely heterogeneous abundances, spanning several orders of magnitude in relative proportion (Fig. S3). Consequently, a substantial proportion of variants are present in low quantities because of uneven sampling of each variant. In an ideal scenario, this distribution would be uniform across the split sites. Second, the sorting process can be error prone, sorting variants into the wrong populations (e.g. a variant that is -GFP will be sorted into +GFP). Third, the sequencing process draws sequencing reads randomly from each population distribution, which introduces intrinsic sampling noise.

To manage these experimental realities, we expanded our workflow and analysis in two directions. First, we used sequencing data not just from Light/+GFP and Dark/+GFP populations, but also Light/-GFP and Dark/-GFP populations. By incorporating these additional populations, we were able to utilize several additional comparisons to double check if a conclusion from a single comparison was the result of an error (Fig. S4). For example, comparing the Light/-GFP to Dark/-GFP may also reveal hits through the absence of variants in the Light/-GFP population. Comparing Light/+GFP to Dark/-GFP can be used to reveal leaky variants. Second, we incorporated Bayesian modeling into our analysis, which assigns phenotypic probabilities to each split site based on sequencing read counts to predict performance of each split (Supplementary Text). Bayesian modeling provides a framework for incorporating all the data from the naïve and sorted populations to produce predictions that combine all the available information, instead of relying on empirical pairwise comparisons between populations. A custom Bayesian model additionally allowed us to explicitly describe the sources of error present in the system, including those that are intrinsic or result from inaccurate observations. Finally, the fact that the results are probabilistic reflects the degree of confidence that one is allowed to expect from a particular dataset: a split site represented in low abundance in the population will result in predictions that do not differ much from the uninformed hypothesis, while an abundant split site might be associated with a more confident prediction.

*Split Cre mapping and validation*

Using our data analysis improvements, we were able to predict the performance of nearly all split sites in the library, resulting in a Cre 'split map' (Fig. 3a). In our Bayesian approach, each split site is designated with a probability for which it will behave as a hit, leaky, or non-functional variant. We noted that our predictions aligned well with known split Cre data from literature. For example, the split at amino acid 59 has been validated as a light-responsive Cre construct with magnets.[21,28] Additionally, a study from Weinberg *et al.* identified multiple functional split sites in the region between 227-277, which align with the general trends we observe in the split map.[7] However, it is important to note that there are differences between the split constructs tested here and reports from the literature. First, a 5-nucleotide duplication caused during the transposon reaction adds two extra amino acids to the C-terminal compared to traditional split proteins (Fig. S1). Also, the expression level and organism likely influence split performance and are specific to each experimental set up.

To assess the quality of the split map predictions, we constructed several individual split Cre variants to test light responsiveness. We built 15 different variants, focusing on predicted hits, but also including some predicted leaky variants, variants where the model prediction was uncertain, and some predicted non-functional variants. Of these 15 variants, we first identified five split sites that were light-responsive (Fig. 3b). Each variant is compared to positive and negative controls of the reporter construct with and without the addition of intact Cre, representing the full range of recombination. Four out of five of these hits—splits at amino acids 153, 154, 229, and 233—were predicted as such. One hit—amino acid 233—was predicted to behave as a non-functional split, however, the model estimated a 22% probability that this split would behave as a hit. When compared to our previously developed split Cre, Opto-Cre-Vvd,[21] split sites 153, 154, 229, and 233 are able to reach higher expression in response to light but display increased dark-state leakiness (Table S5). Second, an additional five constructs were leaky during individual validation experiments (Fig. 3c). In this case, two of five leaky splits were predicted accurately as leaky, while three were predicted to be hits. Therefore, the model is prone to false positives when predicting light responsiveness but performs well when predicting overall catalytic activity. Third, we found constructs that behaved as non-functional variants (Fig. 3d). In this case, five out of five non-functional splits were predicted correctly in the Bayesian analysis.

During the validation process, we uncovered a degree of heterogeneity between colonies. Clonal replicates behaved similarly, as evidenced by good reproducibility between replicates (Fig. 3b-d). However, separate colonies of the variant with the split at amino acid 236, which is a hit, responded differently to light (Fig. S5). Clonal replicates are taken from the same colony after cloning and separated into different cultures during functional testing. Alternatively, separate colonies can be taken during the cloning process and used as separate replicates. In all cases, plasmids were sequenced to verify accurate construction. In the case of 236, one of four colonies displayed a leaky phenotype, while all others were light-responsive. The leaky phenotype may stem from the non-reversible nature of the reporter. If the reporter is activated early during the cloning process, either through an active Cre in the dark state or accidental ambient light exposure, then the +GFP signal will be maintained indefinitely. The heterogeneity in behavior for an individual split may contribute to the prediction errors we encountered when analyzing the sequencing dataset because a given split may behave as several phenotypes. This reality further motivates a Bayesian analysis approach that assigns probabilities instead of making a discrete phenotypic assignment.

Interestingly, areas of catalytic activity, whether leaky or a hit, appear in clusters within the Cre sequence (Fig. 3a). To gain structural understanding, we mapped catalytic activity to the structure of Cre recombinase (Fig. 4a). The functional clusters are primarily in loops between secondary structures, which may be less likely to disrupt protein function. Also, areas of the binding interface between monomers all appear as non-functional variants. In this case, steric hindrance from the dimerization domains may interfere with tetramer formation, rendering the construct non-functional. Notably, four of five clusters appear on one plane of the Cre structure relative to the bound DNA (Fig. 4b). In addition, we plotted catalytic activity of each split site against B-factor, which captures disorder in the crystal structure,[29] however we did not observe a clear correlation with activity indicating it cannot be used to aid functional split site predictions (Fig. S6). Overall, these results demonstrate that our method not only reveals split Cre hits, but supplies holistic protein information for hit, leaky, and non-functional phenotypes that may be useful for informing further engineering of Cre or proteins with similar structure.

## Discussion

Here, we demonstrate a method of creating and screening split protein libraries. With this approach, we provide a technique for incorporating post-translational optogenetic control into proteins without the need for detailed protein engineering expertise or uninformed screening of variants. Our approach can, in principle, be extended to other proteins of interest given cases where it is possible to screen or select for functional variants. Although we focus on light responsiveness, we envision that the experimental workflow and dimer system can be modified to create chemically responsive split proteins, as well.

In this work, we comprehensively screened Cre recombinase split with ‘magnet’ dimers as a proof of concept. In addition to matching trends from previous split Cre studies, we were able to identify several novel light-responsive split sites. We identified intrinsic sources of error in the experimental workflow that contribute to inaccurate predictions when using basic analysis methods. By enhancing our sampling and incorporating a Bayesian model of the experimental error, we make fairly accurate predictions despite these uncertainties in the dataset. We believe this approach to modelling experimental error could extend to other experimental workflows where non-uniform library coverage or incomplete readouts are inherent.

Comprehensively splitting a protein leads to greater structural insight compared to testing only a subset of variants predicted to function. As demonstrated with Cre, data for each amino acid split variant present in the library can be mapped to structure to identify trends. We found that loops distant from a dimer interface are optimal to avoid disruption of recombination activity. Extending our approach to several proteins using various dimerization systems may reveal generalizable rules that could inform split protein engineering strategies. Datasets generated by parallel approaches such as ours could also be used to inform computational methods to improve model accuracy.[22,30,31]

An interesting finding we encountered through validation of individual split constructs was the potential for a split to have heterogenous behaviors between colonies (Fig. S5). Importantly, our prediction model is capable of capturing this variation. It is possible that early expression variation during the cloning process may lead to varying degrees of reporter cutting that are propagated through the validation experiment. Performing the screen with a low-copy plasmid with a more tightly controlled promoter may overcome this issue in the future. Also, we chose the magnet variant nMagHigh1 which contains a kinetic mutation to increase dimer half-life.[20] This may sensitize the library to accidental ambient light exposure, causing validation heterogeneity.

Our method has several limitations. A downside to creating domain insertion libraries with the MuA reaction is that the library distribution is highly heterogeneous, meaning each variant is represented unevenly within the library. Additionally, from a probabilistic standpoint, the majority of the variants produced are not in frame, which decreases sequencing depth. Consequently, our prediction accuracy suffered from false positive predictions of several hits that were found instead to be leaky during validation. Experimental modifications could improve phenotype prediction accuracy. For example, an alternative method for creating domain insertion libraries, called SPINE, uses an oligo library approach instead of transposons.[32] Using SPINE for split protein libraries could produce a higher quality starting library, albeit at a higher cost of library creation. Another limitation of our design is that the split variant is on the same plasmid as the reporter, which is irreversibly recombined. In practice, this means that our system cannot be subjected to multiple successive rounds of sorting and sequencing, a strategy that has been beneficial in other library-based selection approaches.[33] Re-designing the reporter construct so that it is present on a separate plasmid could facilitate multiple rounds of sorting to find enhanced variants. Finally, although we have focused here on inserting the dimers in a configuration where the N-terminus of the protein is followed by dimer domain 1, while dimer domain 2 precedes the C-terminus of the protein, we note that other configurations are possible with straightforward modifications to the construction process (Fig. S7). In the future, it will be interesting to optimize experimental protocols associated with the new split Cre variants we identified, for example by testing different light intensity and duration conditions. There are also potential extensions to our Bayesian modeling approach. The custom Bayesian model is flexible, making it possible to incorporate precise assumptions or expert knowledge about the problem or experimental setup. For example, we modeled the naïve distributions from the light and dark exposed cultures (before sorting) as distinct, but modelling them as a single distribution is also possible. In addition, we heuristically determined values for the false positive and negative rates of the sorting process, but in principle the model could infer values for these rates themselves, albeit at the cost of more difficult numerical evaluation of the posterior.

In summary, this work demonstrates a method to identify functional split sites. Through parallel screening of many split proteins, it allows researchers to confer post-translational control that is agnostic to the protein of interest while requiring little protein engineering expertise and reducing the validation necessary to identify functional variants.

## Methods

### *Strains and plasmids*

We created transposon insertion libraries where the chloramphenicol resistance (Cm$^R$) gene *cat* was inserted randomly in the staging plasmid as described in Nadler *et al*.[24] using the following plasmids with some modifications: pUCKanR-MuA-BsaI (Addgene #79769), pATT-Dest (Addgene #79770), and pTKEI-Dest (Addgene #79784). The following modifications were made to the plasmids from Nadler *et al*. when creating insertion libraries: An mRFP1 sequence from pBbE5c-mRFP1 from the BglBrick library[34] was added to pATT-Dest using golden gate assembly[25] to create pATT-Dest-RFP (Table S1). This provided an easily distinguishable difference in insert size during gel extraction when excising Cre-transposon fragments from the pATT-Dest backbone. The Cre coding sequence was added to pATT-Dest-RFP to create the staging vector pATT-Dest-RFP-Cre (Table S1). The expression plasmid pTKEI-Dest was modified using golden gate assembly[25] to place a Cre GFP reporter into the backbone to create pTKEI-Dest-loxP-sfGFP (Table S1).

The pMag-RBS-nMagHigh1 sequence was introduced on a separate pATT-Dest plasmid to create pATT-BsaI-pMag-nMagHigh1 that contains flanking BsaI sites, GS linkers, and the pMag-RBS-nMagHigh1 sequence (Table S1-S3). The magnet insert was amplified by PCR, followed by a PCR cleanup before being included in a golden gate reaction with the expression library to create the final split protein library. At all steps in the library generation process, colony forming unit (CFU) counts were performed on plates containing appropriate antibiotics to confirm that the number of transformants was $>10^5$ to maintain coverage at least an order of magnitude above the number of possible insertions. A positive control plasmid containing non-split Cre was created by replacing the mRFP1 gene from the BglBrick arabinose inducible vector, pBbS8c-mRFP1, with the Cre coding sequence.[34] Antibiotic concentrations used for plasmid maintenance were 30 μg/mL for kanamycin, 100 μg/mL for carbenicillin, and 25 μg/mL for chloramphenicol.

Plasmids are available via Addgene: https://www.addgene.org/Mary_Dunlop/

*Blue light stimulation*

All light exposure experiments were carried out with a light plate apparatus (LPA)[35] using 465 nm blue light. The split Cre library was cultured in Luria broth (LB) with appropriate antibiotics for plasmid maintenance at 37 °C with 200 rpm shaking and kept in the dark unless being exposed to blue light in the LPA. Overnight cultures of the split Cre library were diluted 1:500 and precultured in the dark for 2 hours. The library was then either kept in the dark or exposed to 100 μW/cm$^2$ blue light for 2 hours followed by 3 additional hours in the dark before being diluted again 1:1000 for overnight growth prior to cell sorting. During validation experiments, single split variants were treated with the same culture and light exposure procedure. pBbS8c-Cre was co-transformed with pTKEI-Dest-loxP-sfGFP to serve as a positive control for Cre activity. Green fluorescence (excitation 480 nm, emission 510 nm) and optical density (OD at 600 nm) readings were taken using a BioTek Synergy H1m plate reader after light induction or dark culturing and overnight growth, as described above.

*Cell sorting*

Fluorescence-activated cell sorting was carried out on a Sony SH800S cell sorter using a 70 μm microfluidic chip. Singlet cells were gated based on GFP fluorescence of pTKEI-Dest-loxP-sfGFP without Cre introduced (reporter only) and pTKEI-Dest-loxP-sfGFP co-transformed with pBbS8c-Cre (reporter + Cre). Gates are shown in Fig. S8. Each culture, either kept in the dark or light exposed, was sorted for 200,000 +GFP cells on ultra-purity mode. A total of six libraries: Light or Dark conditions for +GFP, -GFP, or unsorted (naïve) cultures were miniprepped for sequencing.

*Sequencing and alignment*

Prior to next generation sequencing, each library miniprep was digested with AclI and size-selected through gel extraction to only contain the portion of the plasmid with Cre and inserted magnets. Sequencing libraries were prepared using the Illumina DNA Prep kit, according to manufacturer's specifications. Libraries were then sequenced on an Illumina MiSeq using 2x150 v2 chemistry. Sequencing reads were trimmed of adapters using Trimmomatic[36] v0.39, and a custom Python script was used to identify Cre insertion loci. Out of frame insertions were filtered out and not included in downstream analysis. Splits were indexed (18-343) according to the amino acid sequence in Table S3.

*Bayesian modeling*

The Bayesian approach uses a generative model to map various sources of uncertainty in the experimental process. Each split site can be either a hit (H), leaky (L), or non-functional (N), which are categorical designations. As a prior, for every site i from 1 to 326 (corresponding to amino acids 18-343) we used:

$$site_i \sim Categorical(H\text{: } 2\%,\ L\text{: } 8\%,\ N\text{: } 90\%)$$

This reflects our expectation that most split sites will be non-functional and hits will be comparatively rare. We modeled the distribution of split sites in each naïve library (Dark and Light exposed, pre-sorting) as vectors of non-negative values summing to 1, distributed according to a Dirichlet distribution, which is in good agreement with the sequenced frequencies (Fig. S9):

$$p_D \sim Dirichlet([0.3,\ \ldots,\ 0.3])$$
$$p_L \sim Dirichlet([0.3,\ \ldots,\ 0.3])$$

$p_D$ is the Dark naïve distribution and $p_L$ is the Light naïve distribution. The model accepts the six read count distributions (Light naïve, Dark naïve, Light/+GFP, Light/-GFP, Dark/+GFP, Dark/-GFP) and returns samples from the posterior distribution of the variables to estimate: the 326 $site_i$, $p_D$, and $p_L$. We tally the samples for each $site_i$ to compute hit, leaky, and non-functional probabilities. The Bayesian analysis was modeled and sampled by PyMC, a Python Bayesian inference library.[37] An expanded explanation of our modeling approach is provided in the Supplementary Text.

## Supporting Information

Supplementary tables with plasmid information, sequence information, and sequencing read counts. Supplementary figures with data supporting the manuscript. Supplementary text describing the Bayesian modeling approach.

## Data Availability

All sequence data are available in the Sequence Read Archive, under BioProject PRJNA940279.

## Code Availability

Code used for sequence analysis is available at https://github.com/timplab/tague_splitcre. Code used for Bayesian analysis is available at https://gitlab.com/dunloplab/split-cre-inference.

## Acknowledgments

We thank Dr. Luis Ortiz, Dr. Uros Kuzmanovic, and Dr. James Galagan for training and assistance with the FACS instrument; Michael Sheets for providing a Cre recombinase reporter which we modified for this study; Dr. Dana Nadler for help troubleshooting transposon library creation experiments; and Dr. David Savage and Dr. Stacy Morgan for further assistance related to the transposon library approach. This work was supported by NIH grant R01AI102922 and DOE grant DE-SC0019387.

## Author Contribution

NT conceived and designed the study with input from MJD. NT performed experiments with help from YF for the sequencing studies. For the sequencing studies, WT provided additional input. VA designed and carried out the Bayesian modeling. NT and MJD wrote the manuscript with input from VA and YF.

## Conflict of Interest

The authors declare no competing financial interest.

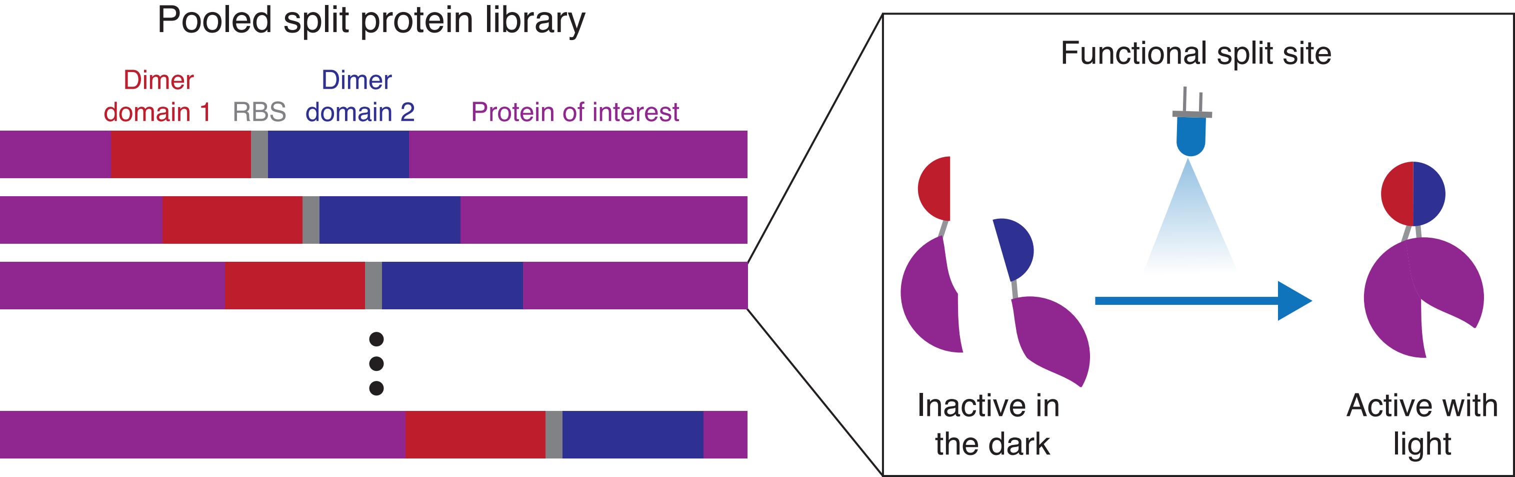
Pooled split protein library
Dimer domain 1
RBS
Dimer domain 2
Protein of interest
Functional split site
Inactive in the dark
Active with light

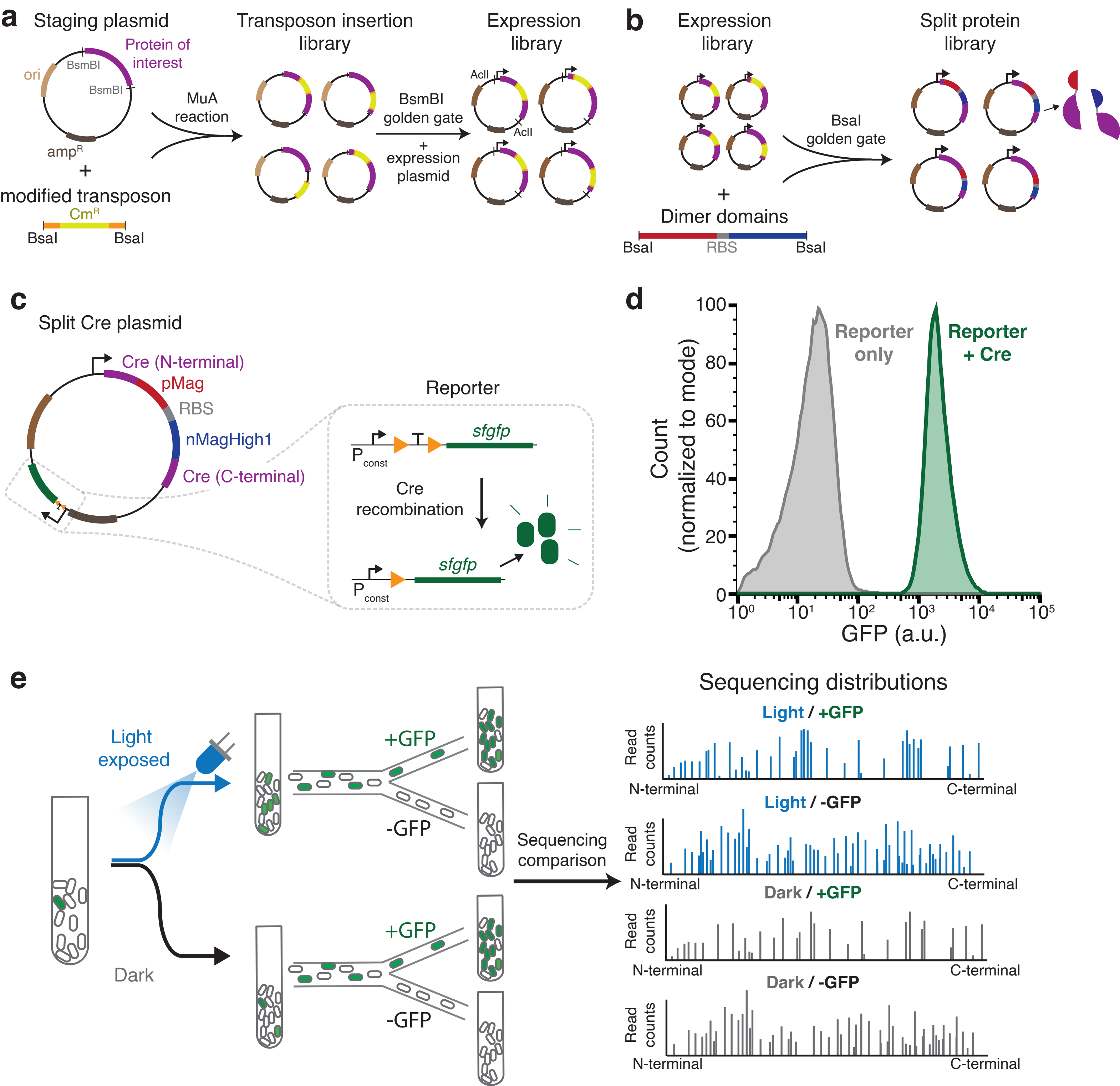
a
Staging plasmid
Protein of interest
ori
BsmBI
BsmBI
amp$^R$
+
modified transposon
Cm$^R$
BsaI
BsaI
MuA reaction
Transposon insertion library
BsmBI golden gate
+ expression plasmid
Expression library
AclI
AclI
b
Expression library
+
Dimer domains
BsaI
RBS
BsaI
BsaI golden gate
Split protein library
c
Split Cre plasmid
Cre (N-terminal)
pMag
RBS
nMagHigh1
Cre (C-terminal)
Reporter
P$_{const}$
sfgfp
Cre recombination
P$_{const}$
sfgfp
d
Count (normalized to mode)
100
80
60
40
20
0
$10^0$
$10^1$
$10^2$
$10^3$
$10^4$
$10^5$
GFP (a.u.)
Reporter only
Reporter + Cre
e
Light exposed
Dark
+GFP
-GFP
+GFP
-GFP
Sequencing comparison
Sequencing distributions
Light / +GFP
Read counts
N-terminal
C-terminal
Light / -GFP
Read counts
N-terminal
C-terminal
Dark / +GFP
Read counts
N-terminal
C-terminal
Dark / -GFP
Read counts
N-terminal
C-terminal

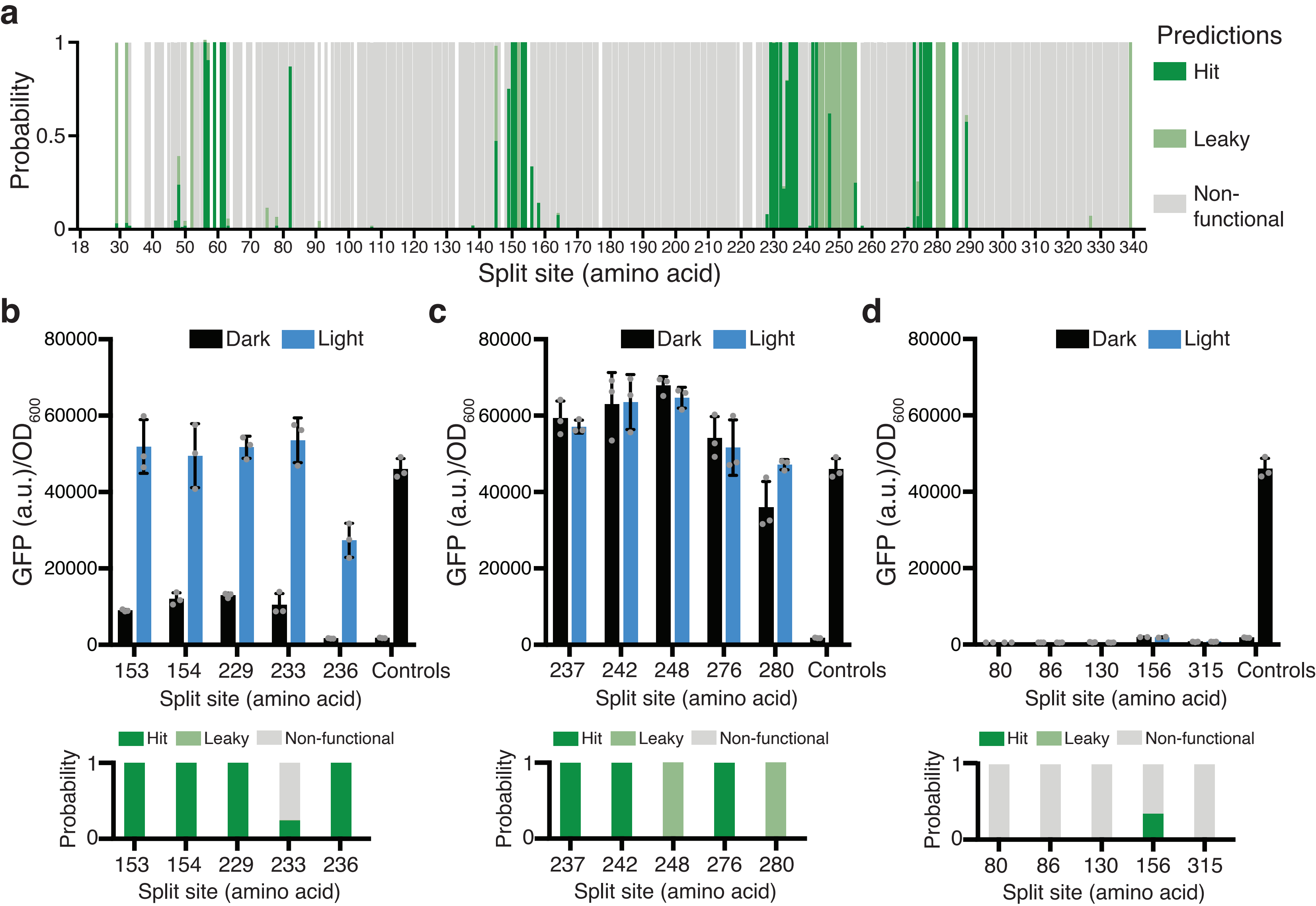
a
Predictions
Hit
Leaky
Non-functional
Probability
1
0.5
0
18
30
40
50
60
70
80
90
100
110
120
130
140
150
160
170
180
190
200
210
220
230
240
250
260
270
280
290
300
310
320
330
340
Split site (amino acid)
b
Dark
Light
GFP (a.u.)/OD600
80000
60000
40000
20000
0
153
154
229
233
236
Controls
Split site (amino acid)
Hit
Leaky
Non-functional
Probability
1
0
153
154
229
233
236
Split site (amino acid)
c
Dark
Light
GFP (a.u.)/OD600
80000
60000
40000
20000
0
237
242
248
276
280
Controls
Split site (amino acid)
Hit
Leaky
Non-functional
Probability
1
0
237
242
248
276
280
Split site (amino acid)
d
Dark
Light
GFP (a.u.)/OD600
80000
60000
40000
20000
0
80
86
130
156
315
Controls
Split site (amino acid)
Hit
Leaky
Non-functional
Probability
1
0
80
86
130
156
315
Split site (amino acid)

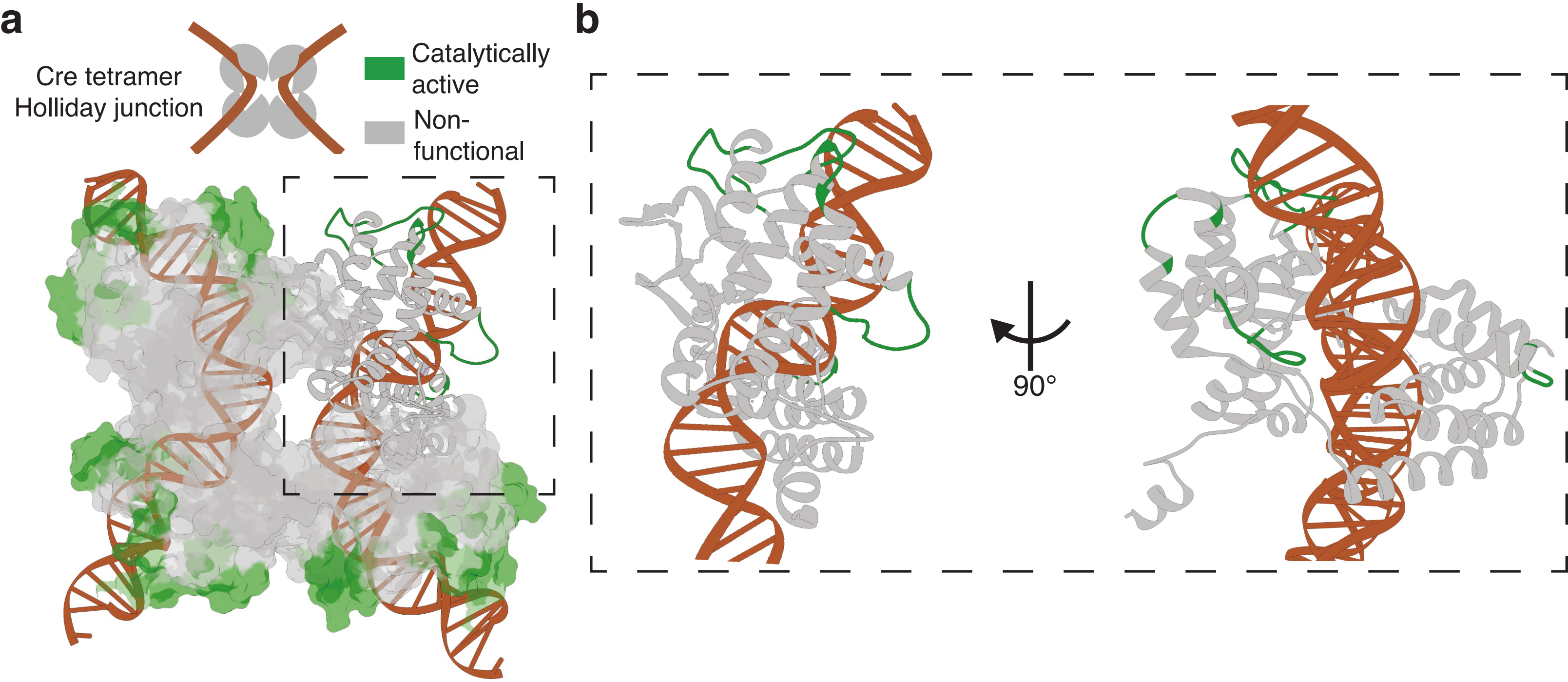
a
Cre tetramer
Holliday junction
🟩 Catalytically active
⬜ Non-functional
b
90°

## References

(1) Feil, R.; Brocard, J.; Mascrez, B.; Lemeur, M.; Metzger, D.; Chambon, P. Ligand-Activated Site-Specific Recombination in Mice. *Proceedings of the National Academy of Sciences of the United States of America* **1996**, *93* (20), 10887–10890. https://doi.org/10.1073/pnas.93.20.10887.

(2) Jullien, N.; Sampieri, F.; Enjalbert, A.; Herman, J. P. Regulation of Cre Recombinase by Ligand-Induced Complementation of Inactive Fragments. *Nucleic acids research* **2003**, *31* (21). https://doi.org/10.1093/nar/gng131.

(3) Olson, E. J.; Tabor, J. J. Post-Translational Tools Expand the Scope of Synthetic Biology. *Current Opinion in Chemical Biology* **2012**, *16* (3–4), 300–306. https://doi.org/10.1016/j.cbpa.2012.06.003.

(4) Davis, K. M.; Pattanayak, V.; Thompson, D. B.; Zuris, J. A.; Liu, D. R. Small Molecule-Triggered Cas9 Protein with Improved Genome-Editing Specificity. *Nature Chemical Biology* **2015**, *11* (5), 316–318. https://doi.org/10.1038/nchembio.1793.

(5) Rose, J. C.; Stephany, J. J.; Valente, W. J.; Trevillian, B. M.; Dang, H. V.; Bielas, J. H.; Maly, D. J.; Fowler, D. M. Rapidly Inducible Cas9 and DSB-DdPCR to Probe Editing Kinetics. *Nature Methods* **2017**, *14* (9), 891–896. https://doi.org/10.1038/nmeth.4368.

(6) Tague, E. P.; Dotson, H. L.; Tunney, S. N.; Sloas, D. C.; Ngo, J. T. Chemogenetic Control of Gene Expression and Cell Signaling with Antiviral Drugs. *Nature Methods* **2018**, *15* (7), 519–522. https://doi.org/10.1038/s41592-018-0042-y.

(7) Weinberg, B. H.; Cho, J. H.; Agarwal, Y.; Pham, N. T. H.; Caraballo, L. D.; Walkosz, M.; Ortega, C.; Trexler, M.; Tague, N.; Law, B.; Benman, W. K. J.; Letendre, J.; Beal, J.; Wong, W. W. High-Performance Chemical- and Light-Inducible Recombinases in Mammalian Cells and Mice. *Nature Communications* **2019**, *10* (1). https://doi.org/10.1038/s41467-019-12800-7.

(8) Dagliyan, O.; Tarnawski, M.; Chu, P. H.; Shirvanyants, D.; Schlichting, I.; Dokholyan, N. V.; Hahn, K. M. Engineering Extrinsic Disorder to Control Protein Activity in Living Cells. *Science* **2016**, *354* (6318), 1441–1444. https://doi.org/10.1126/science.aah3404.

(9) Guntas, G.; Hallett, R. A.; Zimmerman, S. P.; Williams, T.; Yumerefendi, H.; Bear, J. E.; Kuhlman, B. Engineering an Improved Light-Induced Dimer (ILID) for Controlling the Localization and Activity of Signaling Proteins. *Proceedings of the National Academy of Sciences of the United States of America* **2015**, *112* (1), 112–117. https://doi.org/10.1073/pnas.1417910112.

(10) Nihongaki, Y.; Kawano, F.; Nakajima, T.; Sato, M. Photoactivatable CRISPR-Cas9 for Optogenetic Genome Editing. *Nature Biotechnology* **2015**, *33* (7), 755–760. https://doi.org/10.1038/nbt.3245.

(11) Van Haren, J.; Charafeddine, R. A.; Ettinger, A.; Wang, H.; Hahn, K. M.; Wittmann, T. Local Control of Intracellular Microtubule Dynamics by EB1 Photodissociation. *Nature Cell Biology* **2018**, *20* (3), 252–261. https://doi.org/10.1038/s41556-017-0028-5.

(12) Yumerefendi, H.; Lerner, A. M.; Zimmerman, S. P.; Hahn, K.; Bear, J. E.; Strahl, B. D.; Kuhlman, B. Light-Induced Nuclear Export Reveals Rapid Dynamics of Epigenetic Modifications. *Nature Chemical Biology* **2016**, *12* (6), 399–401. https://doi.org/10.1038/nchembio.2068.

(13) Johnson, H. E.; Toettcher, J. E. Signaling Dynamics Control Cell Fate in the Early Drosophila Embryo. *Developmental Cell* **2019**, *48* (3), 361-370.e3.

https://doi.org/10.1016/j.devcel.2019.01.009.

(14) Li, Y.; Zhao, M.; Wei, D.; Zhang, J.; Ren, Y. Photocontrol of Itaconic Acid Synthesis in Escherichia Coli. *ACS Synthetic Biology* **2022**, *11* (6), 2080–2088. https://doi.org/10.1021/acssynbio.2c00014.

(15) Koganezawa, Y.; Umetani, M.; Sato, M.; Wakamoto, Y. History-Dependent Physiological Adaptation to Lethal Genetic Modification under Antibiotic Exposure. *eLife* **2022**, *11*, 1–25. https://doi.org/10.7554/eLife.74486.

(16) Spencer, D. M.; Wandless, T. J.; Schreiber, S. L.; Crabtree, G. R. Controlling Signal Transduction with Synthetic Ligands. *Science* **1993**, *262* (5136), 1019–1024. https://doi.org/10.1126/science.769436.

(17) Tyszkiewicz, A. B.; Muir, T. W. Activation of Protein Splicing with Light in Yeast. *Nature Methods* **2008**, *5* (4), 303–305. https://doi.org/10.1038/nmeth.1189.

(18) Levskaya, A.; Weiner, O. D.; Lim, W. A.; Voigt, C. A. Spatiotemporal Control of Cell Signalling Using a Light-Switchable Protein Interaction. *Nature* **2009**, *461* (7266), 997–1001. https://doi.org/10.1038/nature08446.

(19) Kennedy, M. J.; Hughes, R. M.; Peteya, L. A.; Schwartz, J. W.; Ehlers, M. D.; Tucker, C. L. Rapid Blue-Light-Mediated Induction of Protein Interactions in Living Cells. *Nature Methods* **2010**, *7* (12), 973–975. https://doi.org/10.1038/nmeth.1524.

(20) Kawano, F.; Suzuki, H.; Furuya, A.; Sato, M. Engineered Pairs of Distinct Photoswitches for Optogenetic Control of Cellular Proteins. *Nature Communications* **2015**. https://doi.org/10.1038/ncomms7256.

(21) Sheets, M. B.; Wong, W. W.; Dunlop, M. J. Light-Inducible Recombinases for Bacterial Optogenetics. *ACS Synthetic Biology* **2020**, *9* (2), 227–235. https://doi.org/10.1021/acssynbio.9b00395.

(22) Dagliyan, O.; Krokhotin, A.; Ozkan-Dagliyan, I.; Deiters, A.; Der, C. J.; Hahn, K. M.; Dokholyan, N. V. Computational Design of Chemogenetic and Optogenetic Split Proteins. *Nature Communications* **2018**, *9* (1). https://doi.org/10.1038/s41467-018-06531-4.

(23) Mahdavi, A.; Segall-Shapiro, T. H.; Kou, S.; Jindal, G. A.; Hoff, K. G.; Liu, S.; Chitsaz, M.; Ismagilov, R. F.; Silberg, J. J.; Tirrell, D. A. A Genetically Encoded and Gate for Cell-Targeted Metabolic Labeling of Proteins. *Journal of the American Chemical Society* **2013**, *135* (8), 2979–2982. https://doi.org/10.1021/ja400448f.

(24) Nadler, D. C.; Morgan, S.; Flamholz, A.; Kortright, K. E.; Savage, D. F. Rapid Construction of Metabolite Biosensors Using Domain-Insertion Profiling. *Nature Communications* **2016**, *7* (1). https://doi.org/10.1038/ncomms12266.

(25) Engler, C.; Kandzia, R.; Marillonnet, S. A One Pot, One Step, Precision Cloning Method with High Throughput Capability. *PLoS ONE* **2008**, *3* (11), e3647. https://doi.org/10.1371/journal.pone.0003647.

(26) Nagy, A. Cre Recombinase: The Universal Reagent for Genome Tailoring. *Genesis* **2000**, *26* (2), 99–109. https://doi.org/10.1002/(SICI)1526-968X(200002)26:2<99::AID-GENE1>3.0.CO;2-B.

(27) Meinke, G.; Bohm, A.; Hauber, J.; Pisabarro, M. T.; Buchholz, F. Cre Recombinase and Other Tyrosine Recombinases. *Chemical Reviews* **2016**, *116* (20), 12785–12820. https://doi.org/10.1021/acs.chemrev.6b00077.

(28) Kawano, F.; Okazaki, R.; Yazawa, M.; Sato, M. A Photoactivatable Cre-LoxP Recombination System for Optogenetic Genome Engineering. *Nature Chemical Biology* **2016**, *12* (12), 1059–1064. https://doi.org/10.1038/nchembio.2205.

(29) Sun, Z.; Liu, Q.; Qu, G.; Feng, Y.; Reetz, M. T. Utility of B-Factors in Protein Science: Interpreting Rigidity, Flexibility, and Internal Motion and Engineering Thermostability. *Chemical Reviews* **2019**. https://doi.org/10.1021/acs.chemrev.8b00290.

(30) Leman, J. K.; Weitzner, B. D.; Lewis, S. M.; Adolf-Bryfogle, J.; Alam, N.; Alford, R. F.; Aprahamian, M.; Baker, D.; Barlow, K. A.; Barth, P.; Basanta, B.; Bender, B. J.; Blacklock, K.; Bonet, J.; Boyken, S. E.; Bradley, P.; Bystroff, C.; Conway, P.; Cooper, S.; Correia, B. E.; Coventry, B.; Das, R.; De Jong, R. M.; DiMaio, F.; Dsilva, L.; Dunbrack, R.; Ford, A. S.; Frenz, B.; Fu, D. Y.; Geniesse, C.; Goldschmidt, L.; Gowthaman, R.; Gray, J. J.; Gront, D.; Guffy, S.; Horowitz, S.; Huang, P. S.; Huber, T.; Jacobs, T. M.; Jeliazkov, J. R.; Johnson, D. K.; Kappel, K.; Karanicolas, J.; Khakzad, H.; Khar, K. R.; Khare, S. D.; Khatib, F.; Khramushin, A.; King, I. C.; Kleffner, R.; Koepnick, B.; Kortemme, T.; Kuenze, G.; Kuhlman, B.; Kuroda, D.; Labonte, J. W.; Lai, J. K.; Lapidoth, G.; Leaver-Fay, A.; Lindert, S.; Linsky, T.; London, N.; Lubin, J. H.; Lyskov, S.; Maguire, J.; Malmström, L.; Marcos, E.; Marcu, O.; Marze, N. A.; Meiler, J.; Moretti, R.; Mulligan, V. K.; Nerli, S.; Norn, C.; Ó'Conchúir, S.; Ollikainen, N.; Ovchinnikov, S.; Pacella, M. S.; Pan, X.; Park, H.; Pavlovicz, R. E.; Pethe, M.; Pierce, B. G.; Pilla, K. B.; Raveh, B.; Renfrew, P. D.; Burman, S. S. R.; Rubenstein, A.; Sauer, M. F.; Scheck, A.; Schief, W.; Schueler-Furman, O.; Sedan, Y.; Sevy, A. M.; Sgourakis, N. G.; Shi, L.; Siegel, J. B.; Silva, D. A.; Smith, S.; Song, Y.; Stein, A.; Szegedy, M.; Teets, F. D.; Thyme, S. B.; Wang, R. Y. R.; Watkins, A.; Zimmerman, L.; Bonneau, R. Macromolecular Modeling and Design in Rosetta: Recent Methods and Frameworks. *Nature Methods* **2020**, *17* (7), 665–680. https://doi.org/10.1038/s41592-020-0848-2.

(31) Perrakis, A.; Sixma, T. K. AI Revolutions in Biology. *EMBO reports* **2021**, *22* (11), 1–6. https://doi.org/10.15252/embr.202154046.

(32) Coyote-Maestas, W.; Nedrud, D.; Okorafor, S.; He, Y.; Schmidt, D. Targeted Insertional Mutagenesis Libraries for Deep Domain Insertion Profiling. *Nucleic Acids Research* **2020**, *48* (2), 1–14. https://doi.org/10.1093/nar/gkz1110.

(33) Zhu, L.; McNamara, H. M.; Toettcher, J. E. Light-Switchable Transcription Factors Obtained by Direct Screening in Mammalian Cells. *Nature Communications* **2023**, *14* (1). https://doi.org/10.1038/s41467-023-38993-6.

(34) Lee, T. S.; Krupa, R. A.; Zhang, F.; Hajimorad, M.; Holtz, W. J.; Prasad, N.; Lee, S. K.; Keasling, J. D. BglBrick Vectors and Datasheets: A Synthetic Biology Platform for Gene Expression. *Journal of Biological Engineering* **2011**, *5*, 12. https://doi.org/10.1186/1754-1611-5-12.

(35) Gerhardt, K. P.; Olson, E. J.; Castillo-Hair, S. M.; Hartsough, L. A.; Landry, B. P.; Ekness, F.; Yokoo, R.; Gomez, E. J.; Ramakrishnan, P.; Suh, J.; Savage, D. F.; Tabor, J. J. An Open-Hardware Platform for Optogenetics and Photobiology. *Scientific Reports* **2016**, *6* (November), 1–13. https://doi.org/10.1038/srep35363.

(36) Bolger, A. M.; Lohse, M.; Usadel, B. Trimmomatic: A Flexible Trimmer for Illumina Sequence Data. *Bioinformatics* **2014**, *30* (15), 2114–2120. https://doi.org/10.1093/bioinformatics/btu170.

(37) Abril-pla, O.; Andreani, V.; Carroll, C.; Dong, L.; Fonnesbeck, C. J.; Kochurov, M.; Kumar, R. PyMC : A Modern, and Comprehensive Probabilistic Programming Framework in Python. *PeerJ Computer Science* **2023**, 1–35. https://doi.org/10.7717/peerj-cs.1516.

**Figure Captions**

**Figure 1.** Schematic representation of the split protein library. A protein of interest is split at all potential amino acid sites and screened in parallel to identify functional split sites that are responsive to a specific stimulus. Here, the example of light-inducible dimers is used to illustrate how a split protein can be rendered light-responsive. RBS, ribosome binding site.

**Figure 2**. Generating and screening split protein libraries. **(a)** Method for generating expression libraries with a modified transposon with flanking BsaI restriction enzyme sites. MuA transposase reactions insert the modified transposon containing the chloramphenicol resistance gene ($Cm^R$) randomly into the staging vector containing the gene encoding a protein of interest to create a transposon insertion library. The BsmBI sites are then used for a digestion and gel extraction to isolate the sequence encoding the protein of interest containing a transposon insertion. This fragment is used in a golden gate assembly into the expression vector to generate the expression library. The AclI sites shown are used in a later step to digest the library prior to sequencing. **(b)** The modified transposon in the expression library is replaced by dimerization domains with an internal RBS through a BsaI golden gate reaction to generate a split protein library. **(c)** Each library variant has Cre split by the light-inducible dimers pMag and nMagHigh1. The expression vector for the split Cre library contains a recombinase activity reporter. Cre recombinase excises a transcriptional terminator placed between a constitutive promoter, $P_{const}$, and the gene encoding superfolder GFP, resulting in an increase in fluorescence when Cre is functional. **(d)** Fluorescent histograms of the Cre expression reporter with and without Cre. **(e)** Overview of the experimental workflow used to identify functional split sites within the split Cre library. Libraries are kept in the dark or exposed to 465 nm blue light and sorted based on fluorescence. Sorted libraries are sequenced and compared to distinguish activity of each split site. Library distributions from light exposed and dark populations are compared to uncover individual split site behavior.

**Figure 3**. Cre recombinase split map predictions and validation. **(a)** Phenotypic predictions of split Cre at various amino acid split positions. Each split Cre in the library is assigned a probability of behaving as a hit (dark green), leaky (light green), or non-functional (gray) variant. Split sites that were missing from either naïve library are left white. **(b-d)** Validation of individual split Cre constructs. GFP expression levels with and without exposure to 465 nm blue light are compared to predictions from the library screen to identify true **(b)** hits, **(c)** leaky, or **(d)** non-functional split variants. Controls display GFP expression from the reporter with and without a functional, non-split Cre, representing the full range of recombination. Error bars show standard deviation around the mean (n = 3 or 2 biological replicates; individual data points are overlaid on the bar plot).

**Figure 4.** Split map predictions and protein structure. **(a)** Regions with several residues predicted to be catalytically active when split (hit or leaky, highlighted in green) are mapped to the structure of tetrameric Cre bound to DNA (PDB: 1NZB). Regions highlighted: aa56-62; aa149-154; aa229-237; aa242-255; aa273-286. aa, amino acid. **(b)** Zoomed in structure of a Cre monomer with catalytically active split sites highlighted in green.

# SUPPORTING INFORMATION

# Comprehensive screening of a light-inducible split Cre recombinase with domain insertion profiling

Nathan Tague[1,2], Virgile Andreani[1,2], Yunfan Fan[3], Winston Timp[3,4], Mary J. Dunlop[1,2]*

[1] Department of Biomedical Engineering, Boston University, Boston, MA, USA 02215
[2] Biological Design Center, Boston University, Boston, MA, USA 02215
[3] Department of Biomedical Engineering, Johns Hopkins University, Baltimore, MD, USA
[4] Department of Molecular Biology and Genetics, Johns Hopkins University, Baltimore, MD, USA
* Corresponding author: mjdunlop@bu.edu

## Supplementary Tables

**Table S1**. Plasmids used in this study.

| ***Plasmid*** | ***Origin*** | ***Operon*** | ***Resistance*** | ***Reference*** |
|---|---|---|---|---|
| *pUCKanR-Mu-BsaI* | pMB1 | R1R2(BsaI)-$P_{Cat}$-catR-R2R1(BsaI) | $Cm^R$ | [1] |
| *pATT-Dest-RFP* | pMB1 | $P_{lac}$-lacZ, $P_{lacUV5}$-mRFP1 | $Amp^R$ | This study, derived from [1] |
| *pATT-Dest-RFP-Cre* | pMB1 | cre (BsmBI flanked), $P_{lacUV5}$-mRFP1 | $Amp^R$ | This study |
| *pTKEI-Dest-loxP-sfGFP* | ColE1 | $P_{lac}$-lacZ, $P_{W7}$-loxP-term.-loxP-sfGFP | $Kan^R$ | This study, derived from [1] |
| *pATT-BsaI-pMag-nMagHigh1* | pMB1 | linker-pMag-nMagHigh1-linker (BsaI flanked) | $Amp^R$ | This study |
| *pBbS8c-Cre* | SC101 | $P_{bad}$-cre | $Cm^R$ | This study, derived from pBbS8c-mRFP1 [2] |

**Table S2**. DNA sequences used in this study.

| ***Gene*** | ***Sequence*** |
|---|---|
| *Cre* | gccacctctgatgaagtcaggaagaacctgatggacatgttcagggacaggcaggccttctctgaacacacctggaagatgctcctgtctgtgtgcagatcctgggctgcctggtgcaagctgaacaacaggaaatggttccctgctgaacctgaggatgtgagggactacctcctgtacctgcaagccagaggcctggctgtgaagaccatccaacagcacctgggccagctcaacatgctgcacaggagatctggcctgcctcgcccttctgactccaatgctgtgtccctggtgatgaggagaatcagaaaggagaatgtggatgctggggagagagccaagcaggccctggcctttgaacgcactgactttgaccaagtcagatccctgatggagaactctgacagatgccaggacatcaggaacctggccttcctgggcattgcctacaacaccctgctgcgcattgccgaaattgccagaatcagagtgaaggacatctcccgcaccgatggtgggagaatgctgatccacattggcaggaccaagaccctggtgtccacagctggtgtggagaaggccctgtccctgggggttaccaagctggtggagagatggatctctgtgtctggtgtggctgatgaccccaacaactacctgttctgccgggtcagaaagaatggtgtggctgccccttctgccacctcccaactgtccacccgggccctggaagggatctttgaggccacccaccgcctgatctatggtgccaaggatgactctgggcagagatacctggcctggtctggccactctgccagagtgggtgctgccagggacatggccagggctggtgtgtccatccctgaaatcatgcaggctggtggctggaccaatgtgaacattgtgatgaactacatcagaaacctggactctgagactggggccatggtgaggctgctcgaggatggggac |
| *Magnet insert(linker-pMag-RBS-nMagHigh1-linker)* | gcatcgggttctggaggctcaagcggatcacacactctttacgcccctggaggatacgacattatgggatatttgcggcagattaggaaccgcccaaaccctcaggtcgaactggggcctgtggacacgtcatgtgccctgatcctgtgcgatctgaagcaaaaggacactccgatcgtctacgcctcggaagccttcttgtatatgaccggatacagcaatgcagaggtgctcggcaggaactgcagattcctgcagtcccccgacgggatggtgaaaccaaagtcgactcgcaaatatgtggactcgaacacgatcaacaccatgcggaaggccatcgaccggaacgccgaggtccaggtggaggtggtcaactttaagaagaacggccagcggttcgtgaactttctgaccatgattccggtccgggatgaaaccggagagtacagatactccatgggattccagtgcgaaacagaataagaattcattaaagaggagaaaggtaccatgcatacactttacgctcctgggggctacgacatcatgggctatttggatcagattggcaatcgcccgaatccacaggttgaattagggccagtcgatacgtcgtgcgcactgattttgtgtgatttaaagcaaaaggataccccaattgtttacgcgagtgaggcgtttctgtatatgacgggctactcaaatgcggaggtacttggccgcaactgtcgcttcttacaatcgccggacggcatggtaaagcctaagtcaactcgtaaatacgttgactccaacactatcaatacaattcgcaaagcgatcgatcgcaacgcagaggtccaggtggaggttgttaactttaagaagaatgggcaacgcttcgtgaattttcttacgattattccggttcgtgacgaaaccggcgaatatcgttactctatggggttccagtgtgaaaccgaaggtggcggaggtagcgcgt |
| *Cre reporter ($P_{W7}$-loxP-terminator-loxP-sfGFP)* | ttatcaaaaagagtattgaaataaagtctaacctataggaagattacagccatcgagagggacacggcgaaataacttcgtatagcatacattatacgaagttatccaggcatcaaataaggatccaaactcgagtaaggatctccaggcatcaaataaaacgaaaggctcagtcgaaagactgggcctttcgttttatctgttgtttgtcggtgaacgctctctactagagtcacactggctcaccttcgggtgggcctttctgcgtttataccataacttcgtatagcatacattatacgaagttattttaagaaggagatatacatatgcgtaaaggcgaagagctgttcactggtgtcgtccctattctggtggaactggatggtgatgtcaacggtcataagttttccgtgcgtggcgagggtgaaggtgacgcaactaatggtaaactgacgctgaagttcatctgtactactggtaaactgccggtaccttggccgactctggtaacgacgctgacttatggtgttcagtgctttgctcgttatccggaccatatgaagcagcatgacttcttcaagtccgccatgccggaaggctatgtgcaggaacgcacgatttcctttaaggatgacggcacgtacaaaacgcgtgcggaagtgaaatttgaaggcgataccctggtaaaccgcattgagctgaaaggcattgactttaaagaagacggcaatatcctgggccataagctggaatacaattttaacagccacaatgtttacatcaccgccgataaacaaaaaaatggcattaaagcgaattttaaaattcgccacaacgtggaggatggcagcgtgcagctggctgatcactaccagcaaaacactccaatcggtgatggtcctgttctgctgccagacaatcactatctgagcacgcaaagcgttctgtctaaagatccgaacgagaaacgcgatcatatggttctgctggagttcgtaaccgcagcgggcatcacgcatggtatggatgaactgtacaaataa |

| | |
|---|---|
| *Modified transposon* | tgcatcggagaccgaaaaacgcgaaagcgtttcacgataaatgcgaaaacggatcgatccttttcgaccgaataaatacctgtgacggaagatcacttcgcagaataaataaatcctggtgtccctgttgataccgggaagccctgggccaacttttggcgaaaatgagatgttgatcggcacgtaagaggttccaactttcaccataatgaaataagatcactaccgggcgtattttttgagttgtcgagattttcaggagctaaggaagctaaaatggagaaaaaaatcactggatataccaccgttgatatatcccaatggcatcgtaaagaacattttgaggcatttcagtcagttgctcaatgtacctataaccagaccgttcagctggatattacggcctttttaaagaccgtaaagaaaaataagcacaagttttatccggcctttattcacattcttgcccgcctgatgaatgctcatccggaattacgtatggcaatgaaagacggtgagctggtgatatgggatagtgttcacccttgttacaccgttttccatgagcaaactgaaacgttttcatcgctctggagtgaataccacgacgatttccggcagtttctacacatatattcgcaagatgtggcgtgttacggtgaaaacctggcctatttccctaaagggtttattgagaatatgtttttcgtgtcagccaatccctgggtgagtttcaccagttttgatttaaacgtggccaatatggacaacttcttcgcccccgttttcaccatgggcaaatattatacgcaaggcgacaaggtgctgatgccgctggcgattcaggttcatcatgccgtttgtgatggcttccatgtcggcagaatgcttaatgaattacaacagtactgcgatgagtggcagggcggggcgtaatttttttaaggcagttattggtgcccttaaacgcctggttgctacgcctgaataagtgataataagcggatgaatggcagaaattcgaaagcaaattcgacccggtcgtcggttcagggcagggtcgttaaatagccgcttatgtctattgctggtttaccggtttattgactaccggaagcagtgtgaccgtgtgcttctcaaatgcctgaggccagtttgctcaggctctccccgtggaggtaataattgacgataggatcgatccgttttcgcatttatcgtgaaacgctttcgcgtttttcggtctccgcgtca |

**Table S3**. Amino acid sequences. * Indicates stop codon. (RBS) indicates a ribosome binding site

| ***Protein*** | ***Sequence*** |
|---|---|
| *Cre (indexed 18-343)* | ATSDEVRKNLMDMFRDRQAFSEHTWKMLLSVCRSWAAWCKLNNRKWFPAEPEDVRDYLLYLQARGLAVKTIQQHLGQLNMLHRRSGLPRPSDSNAVSLVMRRIRKENVDAGERAKQALAFERTDFDQVRSLMENSDRCQDIRNLAFLGIAYNTLLRIAEIARIRVKDISRTDGGRMLIHIGRTKTLVSTAGVEKALSLGVTKLVERWISVSGVADDPNNYLFCRVRKNGVAAPSATSQLSTRALEGIFEATHRLIYGAKDDSGQRYLAWSGHSARVGAARDMARAGVSIPEIMQAGGWTNVNIVMNYIRNLDSETGAMVRLLEDGD |
| *Magnet insert* (*linker*-pMag-*RBS*-nMagHigh1-*linker*) | ASGSGGSSGSHTLYAPGGYDIMGYLRQIRNRPNPQVELGPVDTSCALILCDLKQKDTPIVYASEAFLYMTGYSNAEVLGRNCRFLQSPDGMVKPKSTRKYVDSNTINTMRKAIDRNAEVQVEVVNFKKNGQRFVNFLTMIPVRDETGEYRYSMGFQCETE * *(RBS)* MHTLYAPGGYDIMGYLDQIGNRPNPQVELGPVDTSCALILCDLKQKDTPIVYASEAFLYMTGYSNAEVLGRNCRFLQSPDGMVKPKSTRKYVDSNTINTIRKAIDRNAEVQVEVVNFKKNGQRFVNFLTIIPVRDETGEYRYSMGFQCETEGGGGSAS |

**Table S4.** Read counts associated with each split site for each of the six sequenced libraries. In all cases, data are listed sequentially for splits indexed 18-343 according to the amino acid sequence in Table S3.

*Data are provided in Table_S4.xlsx*

**Table S5.** Comparison of hits from this study to Opto-Cre-Vvd from *Sheets, et al.*[3], normalized to respective reporter controls, with the negative and positive control values representing 0 and 1, respectively.

| Split Cre variant | Dark<br>(fluo. normalized) | Light<br>(fluo. normalized) | Source |
|---|---|---|---|
| Opto-Cre-Vvd | 0.03 | 0.86 | S*heets, et al.*[3] |
| 153 | 0.16 | 1.13 | This study |
| 154 | 0.23 | 1.08 | This study |
| 229 | 0.25 | 1.13 | This study |
| 233 | 0.20 | 1.17 | This study |
| 236 | 0.00 | 0.58 | This study |

## Supplementary Figures

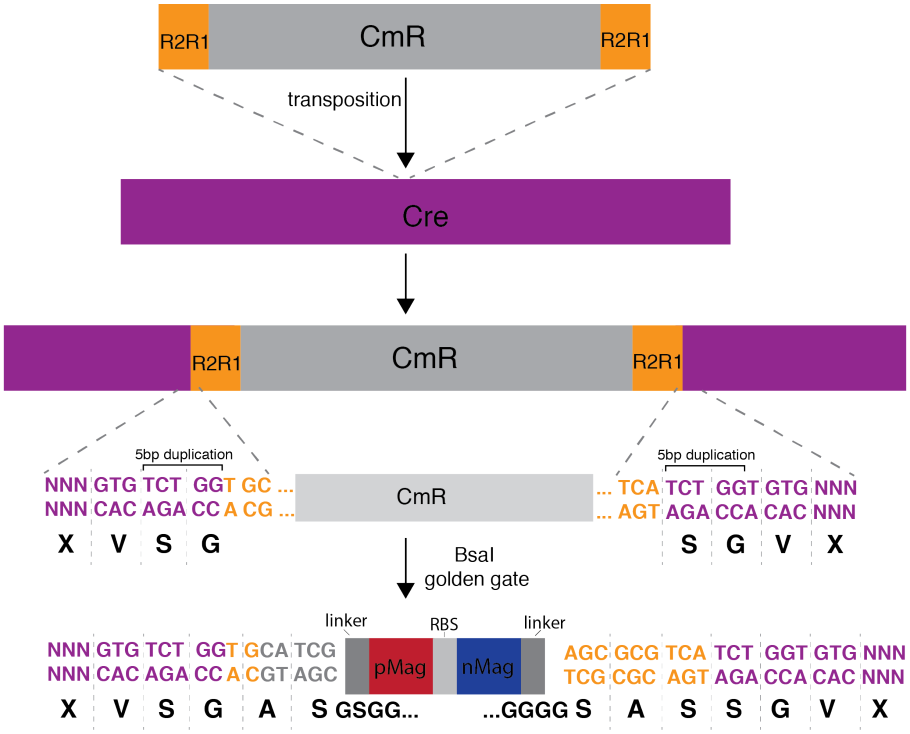

**Figure S1**. Schematic of transposon insertion. MuA-mediated transposition results in a 5 nucleotide duplication of the Cre sequence and addition of a 2 nucleotide scar on the 5' and 3' ends of the transposon. Replacement of the transposon with the magnet dimer domains through a BsaI golden gate maintains the open reading frame with flexible linkers connecting N- and C-terminal fragments of Cre with pMag and nMagHigh1, respectively. R2R1 sites are sequences recognized by MuA transposase and necessary for transposition.

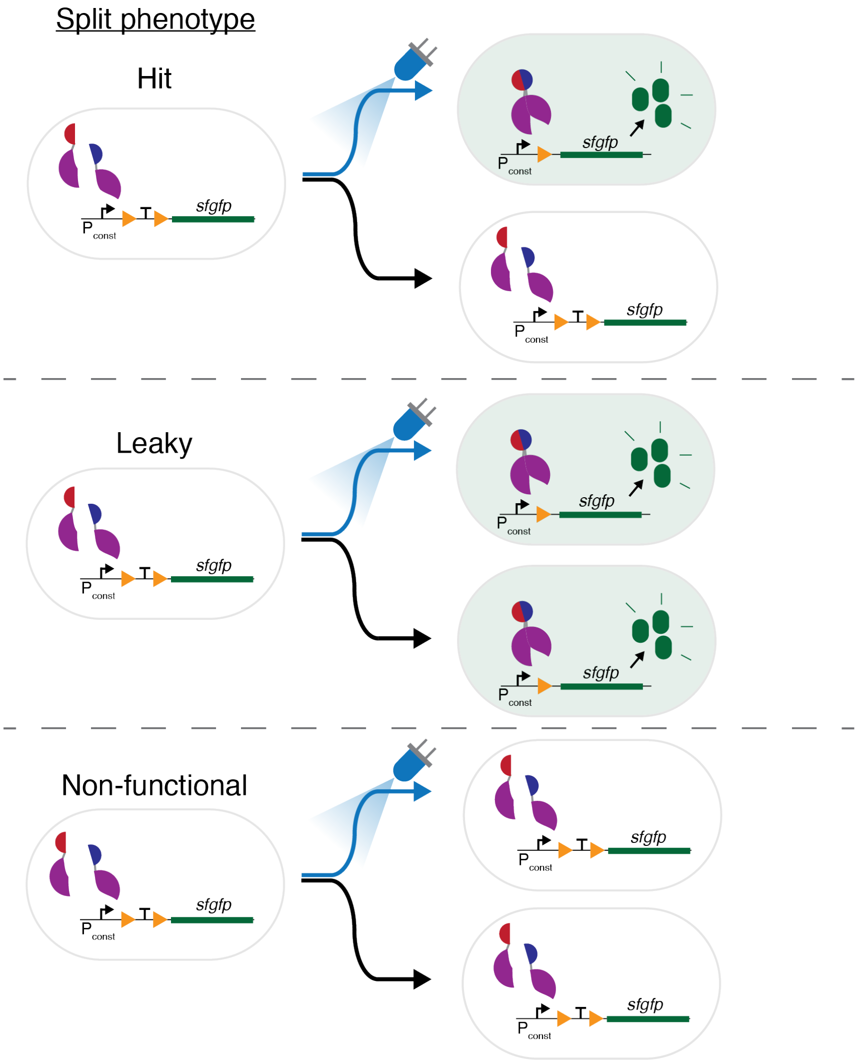

**Figure S2**. A split Cre construct can function as one of three phenotypes using the GFP Cre reporter: 1) Hit: Cre recombinase activity is light responsive. 2) Leaky: Cre is active even in the dark, 3) Non-functional: Cre is inactive in dark and light conditions.

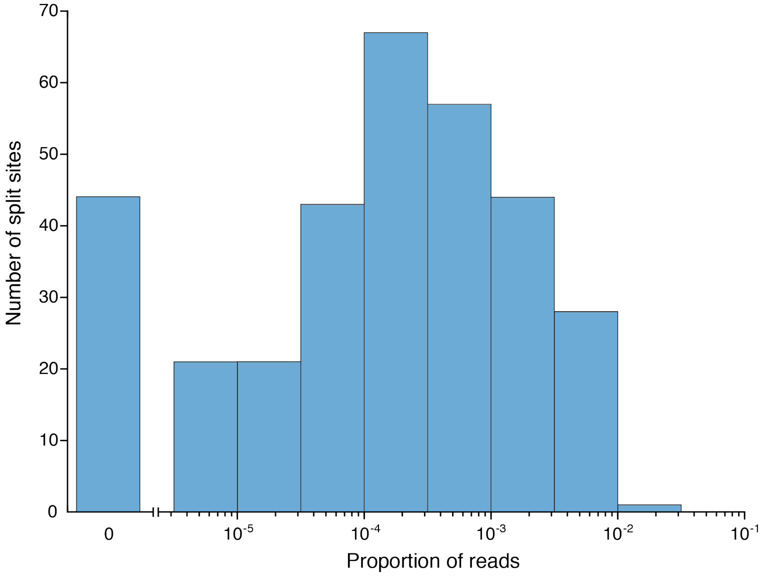

**Figure S3**. Distribution of split sites in the Light-exposed naïve library prior to fluorescent activated cell sorting.

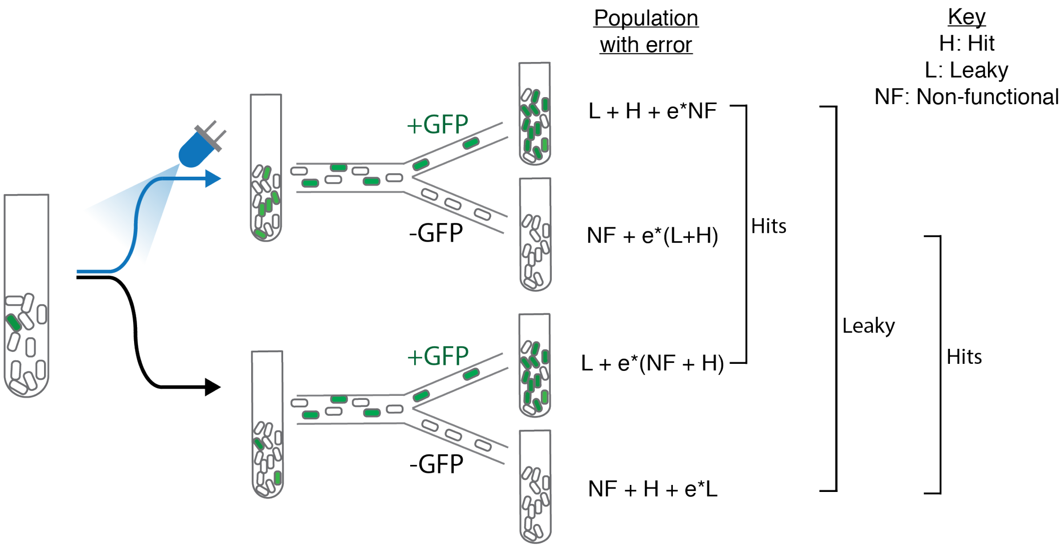

**Figure S4**. Schematic detailing the makeup of split phenotypes expected to be present in each population after sorting. Sorting error, e, leads to spurious events, e.g. non-functional splits present in the +GFP populations. Three ratio comparisons of the resulting distributions can be used to extract information from the libraries to overcome variation stemming from sorting errors and under sampled variants. Light/+GFP compared to Dark/+GFP will reveal hits, Light/+GFP compared to Dark/-GFP provides information about possible leaky variants, and Light/-GFP compared to Dark/-GFP will reveal hits.

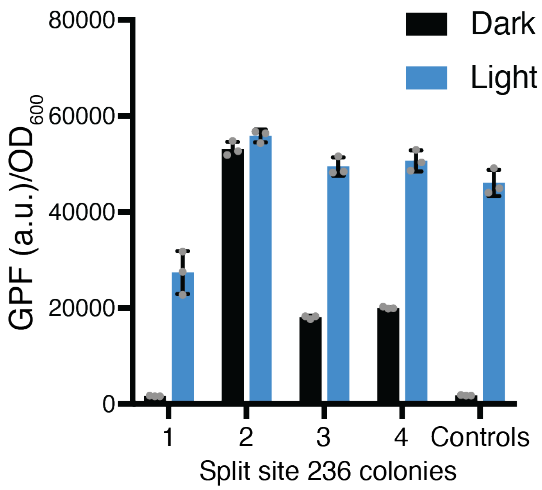

**Figure S5**. GFP expression levels with and without exposure to 465 nm blue light in four colonies of split Cre 236 tested in parallel. Controls display sfGFP expression from the reporter with and without the addition of functional, non-split Cre. Error bars show standard deviation around the mean (n = 3 replicates).

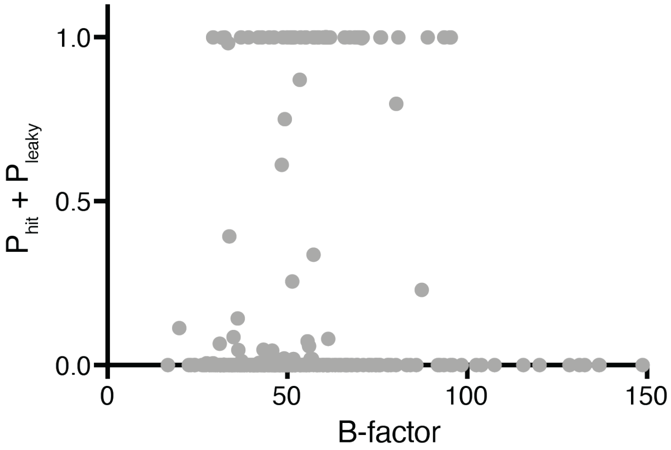

**Figure S6**. Probability of catalytic activity (hit or leaky) plotted against B-factor for residues in the Cre structure (PDB: 1NZB).

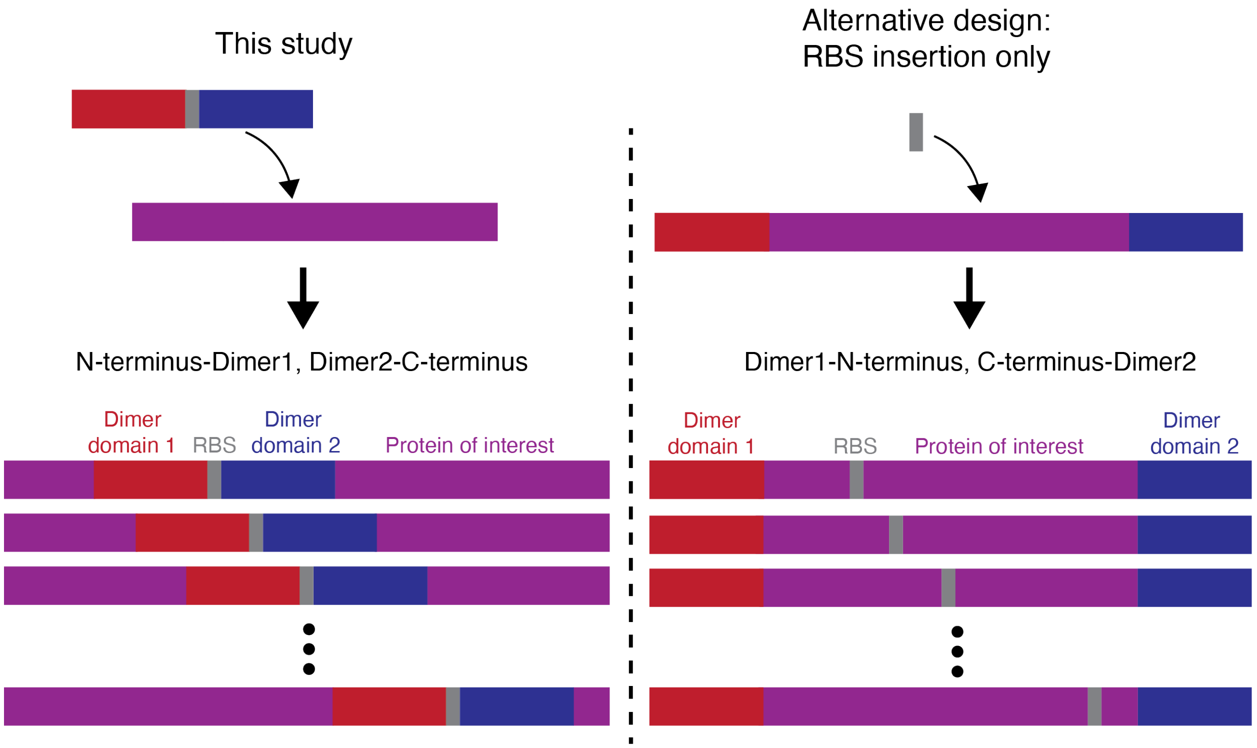

**Figure S7.** Alternative library construction design. In this study, the inserted fragment consists of Dimer1-RBS-Dimer2, which results in the following configuration: N-terminus-Dimer1, Dimer2-C-terminus. By instead flanking the protein of interest with the dimer domains and only inserting an RBS fragment, an alternative configuration can be created as follows: Dimer1-N-terminus, C-terminus-Dimer2.

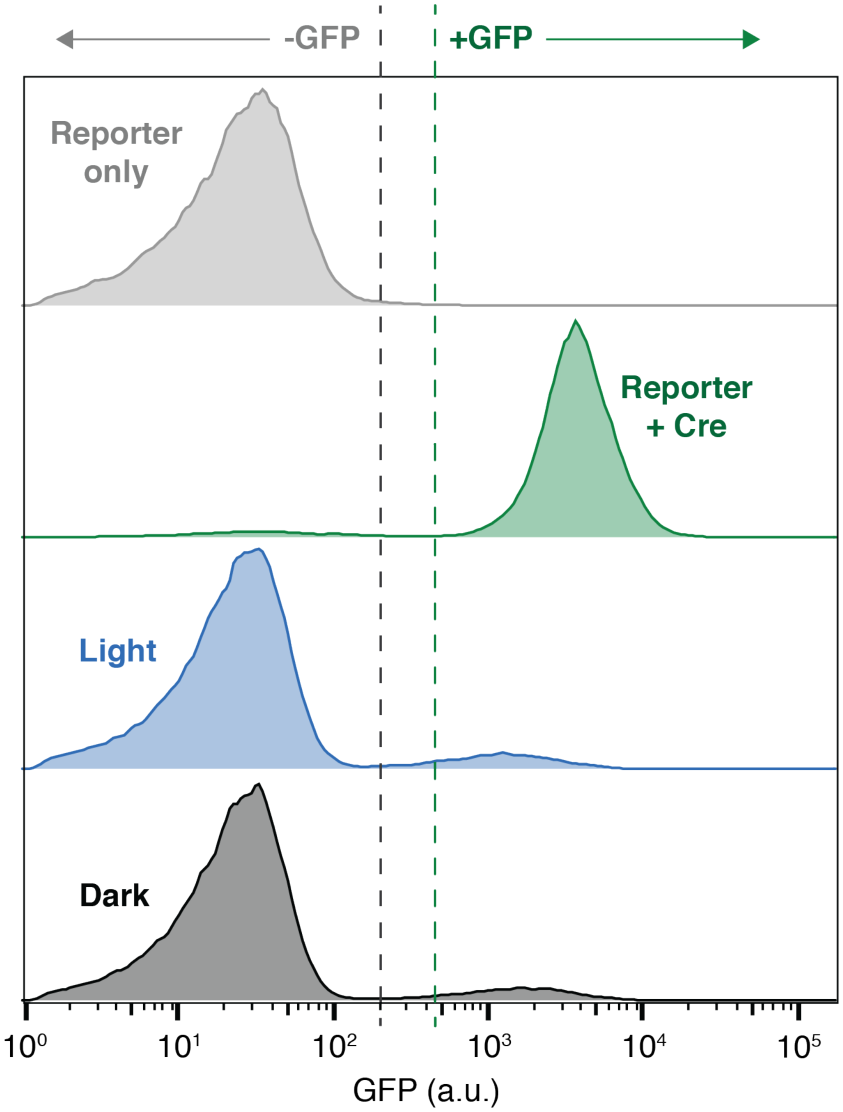

**Figure S8.** Sorting gates used for -GFP and +GFP cell sorting. Cells containing the reporter only or the reporter plus a non-split Cre were used as negative and positive controls, respectively, to set gating thresholds. Light exposed and Dark library GFP distributions are shown and were sorted using these thresholds.

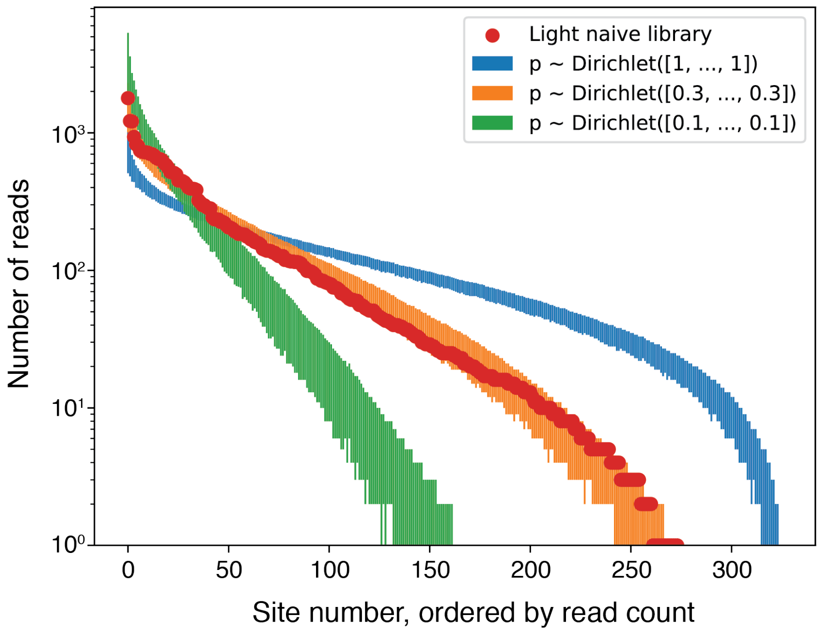

**Figure S9.** Choosing a Dirichlet prior of parameter [0.3, … , 0.3] for the Light-exposed naïve library distribution reproduces the experimentally observed dispersion well. The bars represent the 94% highest-density interval of the simulated results.

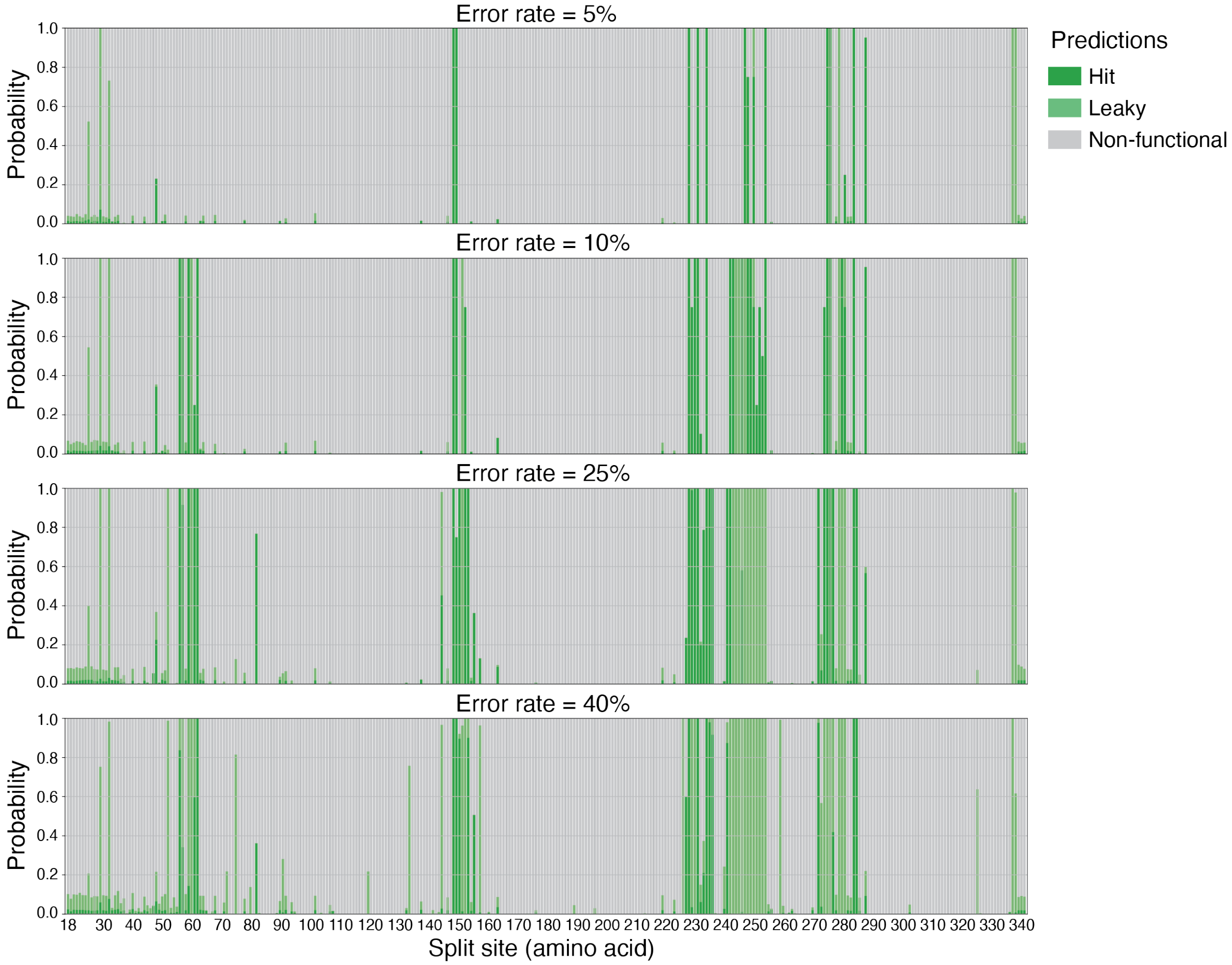

**Figure S10.** Sensitivity of the analysis results to the values of the false positive and false negative sorting error rates. Error rates (top to bottom): 5%, 10%, 25%, and 40%. Note that 25% is the value used in Fig. 3a. Low error rates are more selective; with high error rates the model to labels more sites as active. Note that 50% error rate case corresponds to a degenerate case where cells are sorted randomly, independently of the GFP expression.

## Supplementary Text – Bayesian Modeling

### *Bayesian modeling*

We developed the statistical model as a generative model, i.e. a mapping in probabilistic terms of our knowledge of the experimental process. The experiment is highly random, and every step creates a probability distribution related to some of the previous distributions. The model creates the distributions and describes how they relate to each other.

### *Nature of the split sites*

Every site $i \in [1, 326]$ (corresponding to amino acids 18-343) can be a hit (H), leaky (L), or non-functional (N) variant. This is described by a categorical distribution. We give prior probabilities to H, L, and N according to the proportions: 2% hits, 8% leaky, and 90% non-functional, which is based on empirical observations.

$$site_i \sim \text{Categorical}(H : 2\%, L : 8\%, N : 90\%)$$

### *Distribution of the naïve populations*

The split sites are generated by a random process with a non-uniform distribution. We adapted the Dirichlet probability distribution to describe a prior over this initial split site distribution. The parameter of a Dirichlet distribution is a vector of N numbers, where N is the number of categories (here 326 possible split sites). Because we do not want to favor any split site a priori, we leave all 326 numbers equal to the same value, the only adjustment being the shared value $\alpha$. We create two naïve distributions: $p_L$ for the Light-exposed naïve library, and $p_D$ for the Dark-exposed naïve library.

$$p_{L,D} \sim \text{Dirichlet}\ ([\alpha, \dots, \alpha])$$

Modeling the plasmid sequencing process as a multinomial sampling over the naïve library, we can describe the naïve light and dark read counts as follows, where $N$ is the total number of read counts (sequencing depth):

$$(L, D) \sim \text{ Multinomial } (N, p_{L,D})$$

Where L and D are vectors of 326 length with read counts corresponding to the abundance of a given variant. This allows us to simulate read counts that we would observe from Dirichlet-distributed naïve distributions (Fig. S9). Comparing these simulations to experimental data allowed us to determine an appropriate value for $\alpha$, where $\alpha$ = 0.3 reproduces the dispersion observed experimentally in the sequencing of the naïve libraries well.

### *Sorting process*

The sorting process happens independently for every cell that passes through the cell sorter.

Light-treated cells that behave as hits (H) or leaky (L) are sorted as +GFP with a probability $1 - fn$, and -GFP with a probability $fn$, where $fn$ is the false negative rate. Inversely, light-treated cells that behave as non-functional (N) are sorted as +GFP with a probability $fp$, and -GFP with a probability $1 - fp$, where $fp$ is the false positive rate. We fixed both $fn$ and $fp$ at 25%, following empirical sorting observations. This is however a very conservative estimate, and the results were not significantly affected by setting these rates to other values between 3% and 40% (Fig. S10). Note that the closer these error rates are to 50%, the less information is learned from the experiment and at 50%, the posterior will be identical to the prior.

Introducing $(s_L^{+,-})_i$ the probability that a split site at position $i$ and Light-exposed gets sorted as +,-GFP, we can write

$$(s_L^+)_i = \begin{cases} 1 - \text{fn} & \text{if sites}_i = L \text{ or } H \\ \text{fp} & \text{if sites}_i = N \end{cases}$$

and

$$(s_L^-)_i = 1 - (s_L^+)_i$$

Similarly, for the Dark-exposed population,

$$(s_D^+)_i = \begin{cases} 1 - \text{fn} & \text{if sites}_i = L \\ \text{fp} & \text{if sites}_i = N \text{ or } H \end{cases}$$

and

$$(s_D^-)_i = 1 - (s_D^+)_i$$

From there, we derive the proportions of each cell type in the four sorted populations. For split site $i$:

$$(p_{L,D}^{+,-})_i = \frac{(p_{L,D})_i (s_{L,D}^{+,-})_i}{\sum_j (p_{L,D})_j (s_{L,D}^{+,-})_j}$$

This allows us to finally express the sequencing results of the four sorted populations:

$$(L, D)^{+,-} \sim \text{ Multinomial } (N, p_{L,D}^{+,-})$$

*Model implementation*

We implemented the model in Python, with the PyMC library.[4] The crux of the implementation is as follows:

```
with pm.Model():
    # 0 = H, 1 = L, 2 = N
    sites = pm.Categorical("sites", [p_hit, p_leaky, 1-p_hit-p_leaky], size=326)
    p_l = pm.Dirichlet("p_l", [alpha] * 326)
    p_d = pm.Dirichlet("p_d", [alpha] * 326)
    pm.Multinomial("L", n=sum(df.light), observed=df.light)
    pm.Multinomial("D", n=sum(df.dark), observed=df.dark)
    s_l = pm.math.stack([1 - fn_rate, 1 - fn_rate, fp_rate])[sites]
    pm.Multinomial("L+", n=sum(df.light_pos),
        p=p_l * s_l / (p_l * s_l).sum(), observed=df.light_pos)
    pm.Multinomial("L-", n=sum(df.light_neg),
        p=p_l * (1 - s_l) / (p_l * (1 - s_l)).sum(), observed=df.light_neg)

s_d = pm.math.stack([fp_rate, 1 - fn_rate, fp_rate])[sites]
pm.Multinomial("D+", n=sum(df.dark_pos),
    p=p_d * s_d / (p_d * s_d).sum(), observed=df.dark_pos)
pm.Multinomial("D-", n=sum(df.dark_neg),
    p=p_d * (1 - s_d) / (p_d * (1 - s_d)).sum(), observed=df.dark_neg)
```

*Inference*

We ran 4 Markov chain Monte Carlo simulations of 10,000 samples each, preceded by a phase of burn-in/tuning of the same length.

## Supplementary References

(1) Nadler, D. C.; Morgan, S.; Flamholz, A.; Kortright, K. E.; Savage, D. F. Rapid Construction of Metabolite Biosensors Using Domain-Insertion Profiling. *Nature Communications* **2016**, *7* (1). https://doi.org/10.1038/ncomms12266.

(2) Lee, T. S.; Krupa, R. A.; Zhang, F.; Hajimorad, M.; Holtz, W. J.; Prasad, N.; Lee, S. K.; Keasling, J. D. BglBrick Vectors and Datasheets: A Synthetic Biology Platform for Gene Expression. *Journal of Biological Engineering* **2011**, *5*, 12. https://doi.org/10.1186/1754-1611-5-12.

(3) Sheets, M. B.; Wong, W. W.; Dunlop, M. J. Light-Inducible Recombinases for Bacterial Optogenetics. *ACS Synthetic Biology* **2020**, *9* (2), 227–235. https://doi.org/10.1021/acssynbio.9b00395.

(4) Abril-pla, O.; Andreani, V.; Carroll, C.; Dong, L.; Fonnesbeck, C. J.; Kochurov, M.; Kumar, R. PyMC : A Modern, and Comprehensive Probabilistic Programming Framework in Python. *PeerJ Computer Science* **2023**, 1–35. https://doi.org/10.7717/peerj-cs.1516.